Tempering effects in a normalized hot forged Cu-Zn-Al shape memory alloy

G. VITEL[a], A. L. PARASCHIV[b], M. G. SURU[b], N. CIMPOEŞU[b], L.-G. BUJOREANU[b]*

[a] *"Axinte Uricariul" School, 707425 Scânteia, jud. Iaşi, Romania*
[b] *The "Gheorghe Asachi" Technical University from Iaşi, Bd. D. Mangeron 67, 700050 Iaşi, Romania*

A normalized hot forged Cu-15Zn-6Al (mass. %) shape memory alloy (SMA) was subjected to tempering heat treatments meant to enhance the reversion to parent phase (austenite) of thermally induced martensite. By means of differential scanning calorimetry (DSC) the reversibility of martensitic transformation was verified during constant-rate heating-cooling cycles. The results have showed that 373 K- tempering destabilized martensite and enabled its reversion at lower temperatures, on heating. Conversely, 473 K-tempering caused the disappearance of martensite phase. The structural features, observed both by optical microscopy (OM) and by scanning electron microscopy (SEM), at the phase transformation product obtained after 473 K-tempering suggest the presence transitory bainite, since its nucleation is diffusionless while its growth is diffusion controlled, which could explain the lack of reversibility.

1. Introduction

Commercial shape memory alloys (SMAs) include Cu-Zn-Al base alloy, characterized by recovery strains and stresses as large as 4 % and 400 MPa, respectively [1].

The main drawback in exploiting Cu-Zn-Al base SMAs, as functional materials, is diffusion-controlled martensite stabilization, occurring during successive heating even in low temperature rage [2] and causing the shift of the critical temperatures for reverse martensitic transformation (A_s and A_f) to higher temperatures [3].

In the case of a martensitic Cu-Zn-Al SMA subjected to thermal cycling with free-air cooling, thermal memory degradation was associated with an alteration of martensite reversion to parent phase [4]. On the other hand, no alteration of reverse martensite transformation was reported in the case of a homogenized Cu-Zn-Al SMA subjected to tempering heat treatments up to 573 K [5].

These reports suggest that thermal memory behaviour is strongly dependent on heat treatment (HT) state of SMAs, particularly in the case on Cu-Zn-Al system. Consequently, the present paper aims to emphasize tempering effects on the thermal memory behaviour of a normalized Cu-Zn-Al SMA, by corroborating calorimetric data with microscopic features.

2. Experimental details

The present experiments employed, as a raw material, normalized hot forged plates of Cu-15 Zn-6 Al (mass. %) SMA processed as previously mentioned [6, 7].

The complete diagram of the thermomechanical processing of the alloy under study is shown in Fig.1. The first treatment corresponds to 1023K - hot forging, the

primary HT is normalization (18 ks/ 1073K/ air) and the secondary HT is tempering (300s/ 373; 473 K/ air).
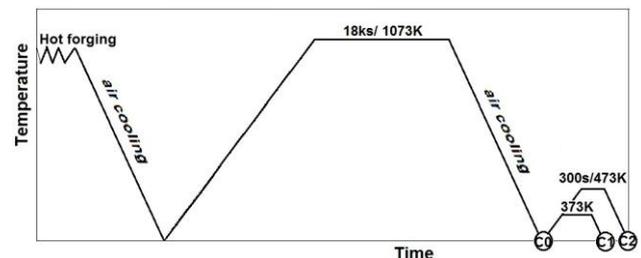
Fig. 1 Thermomechanical processing diagram of Cu-15Zn-6Al SMA. C0-normalized specimen; C1-specimen tempered at 373K; C2-specimen tempered at 473K.

From normalized (C0) and tempered (C1, C2) specimens, after careful mechanical removal under water cooling of any marks of superficial corrosion, three fragments weighing less than 50×10^{-6} kg each were cut, with appropriate caution in order not to alter their thermal histories.

The fragments were analysed by means of a NETZSCH differential scanning calorimeter type DSC 200 F3 Maya, with sensitivity: < 1μW, temperature accuracy: 0.1 K and enthalpy accuracy: generally < 1%. The device was calibrated with Bi, In, Sn and Zn standards. Each thermal cycle comprised: (i) heating, under Ar protective atmosphere, with 1.67×10^{-1} K·sec^{-1} up to 473 K; (ii) isothermal maintaining for 180 sec; (iii) cooling to 373 K, by means of liquid nitrogen, with a cooling rate of 1.67×10^{-1} K·sec^{-1}; (iv) isothermal maintaining for 180 sec and (v) final heating to 473 K, under Ar protective atmosphere, with 1.67×10^{-1} K·sec^{-1}.

The experiments were performed by using corresponding correction curves and the results were evaluated with PROTEUS software, provided by the producer, by using sigmoid-type baselines.

In order to reveal the structural effects of tempering on C0 normalized specimen, other fragments were cut from respective raw specimens C0, C1 and C2, under appropriate water cooling, meant to avoid any alteration of their thermal histories. Each of the fragments were was encapsulated into Mécaprex KM-U could mounting resign, before being ground up to 2400 mesh and automatically polished for 1.8 ks, on a Metkon FORCIPOL 1V machine, with 0.04 μ Alumine Suspension. Etching was applied with 30 % HNO_3 aqueous solution.

The three metallographically prepared specimens, C0, C1 and C2, were analyzed by optical microscopy (OM), using a Meiji TECHNO device with video camera and QCapture software and by scanning electron microscopy (SEM), using a SEM—VEGA II LSH TESCAN microscope, coupled with an EDX—QUANTAX QX2 ROENTEC detector.

3. Experimental results and discussion

The first DSC thermograph, corresponding to thermal cycling of normalized specimen C0, is shown in Fig. 2.
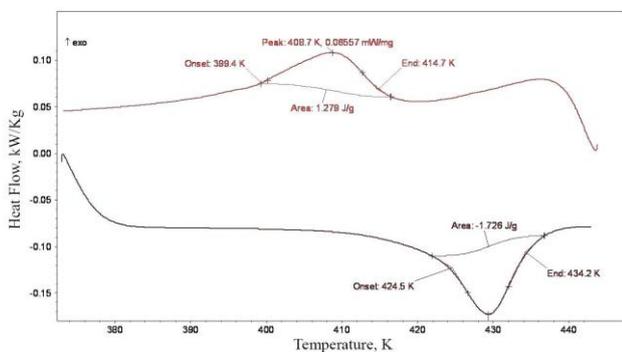
Fig. 2. DSC thermograph of normalized specimen C0, during a cooling-heating cycle, between 373 and 473 K, with 1.67×10^{-1} K•sec^{-1}.

According to previous reports [4, 5, 8], the exothermic peak occurring on cooling corresponds to forward (direct) martensite transformation between $M_s=414.7$ K and $M_f=399.4$K. The transformation of parent phase (austenite) [9] into thermally induced martensite is accompanied by a specific energy release $\Delta H^{A \to M} \cong 1.3$ kJ/ kg. During heating, the newly formed thermally induced martensite reverts to austenite by means of an endothermic transition associated with the lower peak in Fig. 2. This reverse martensitic transformation is characterized by $A_s=424.5$K and $A_f=434.2$K, being accompanied by a specific energy absorption $\Delta H^{M \to A} \cong 1.7$ kJ/kg.

The second DSC thermogram corresponds to tempered specimen C1 and is shown in Fig. 3.

In this case, as well, the transformation is reversible but critical transformation temperatures are slightly shifted to lower values. Martensite formed between $M_s=406.6$ K and $M_f=395$K and reverted to austenite between $A_s=418.7$K and $A_f=427.1$K. On the other hand, specific energy variations were much higher than for normalized specimen: $\Delta H^{A \to M} \cong 2.26$ kJ/ kg and $\Delta H^{A \to M} \cong 4.423$ kJ/ kg.
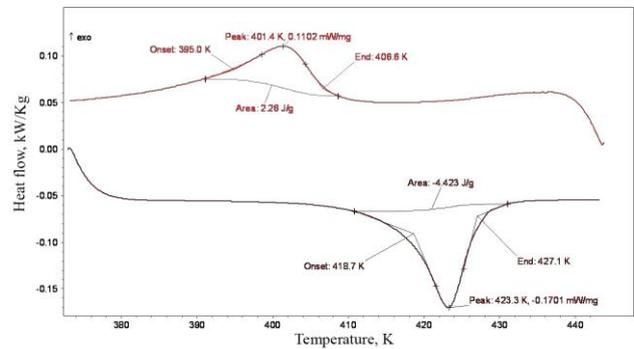
Fig. 3. DSC thermograph of tempered specimen C1 during a cooling-heating cycle, between 373 and 473 K, with 1.67×10^{-1} K•sec^{-1}.

These data suggest the fact that both the C0 normalized specimen and the C1 tempered specimen were martensitic at room temperature, at 300K, since direct martensitic transformation ended at 395 K. Apparently, tempering destabilized thermally induced martensite and for this reason all critical temperatures of martensitic transformation have been lower, with 4.4-8 K, at C1 tempered specimen as compared to C0 normalized specimen.

The third DSC thermograph was recorded with the fragment cut from specimen C2, tempered at 473 K and is illustrated in Fig. 4.
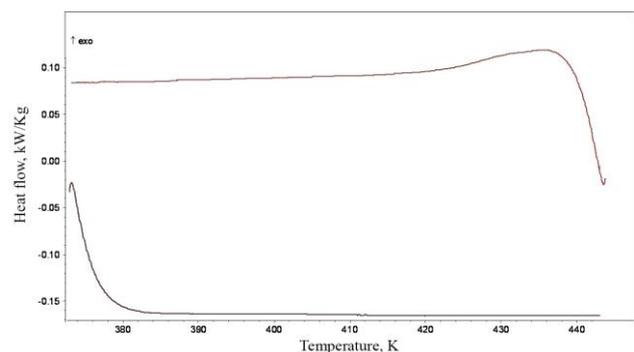
Fig. 4. DSC thermograph of tempered specimen C2, during a cooling-heating between 373 and 473 K, with 1.67×10^{-1} K•sec^{-1}.

Obviously, there is no sign of solid state transition, between 373 and 473 K, neither on cooling nor on heating. No martensite was formed on cooling and no pre-existing martensite reverted to austenite on heating.

For a better inside on the initial structure of the specimens, microscopic observations were performed both optically (OM) and electronically (SEM). The first results are shown in Fig. 5, illustrating a typical OM micrograph

of normalized specimen C0.

It is rather evident that the structure comprises short martensite plates with diamond-like aspect [10]. It is expectable that, during initial heating, these martensite plates revert to austenite, which is the starting or parent phase for the thermal cooling-heating cycle, illustrated in Fig.2. During cooling austenite transforms to martensite which reverts to austenite during subsequent heating. This is the thermodynamic mechanism responsible for thermal memory behaviour. Conversely, the alteration/ absence of martensite reversion to austenite on heating is associated with *amnesia* [11].
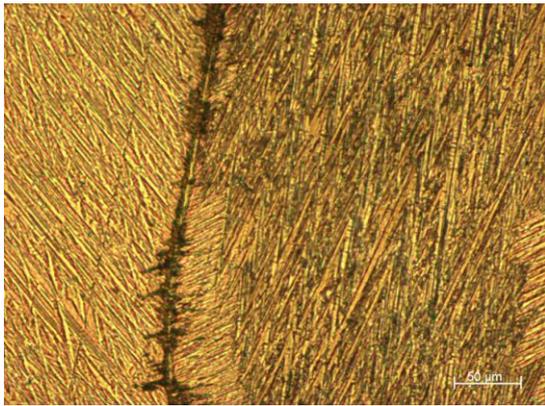
Fig. 5. OM micrograph of normalized specimen C0, revealing short martensite plates with diamond structure.

The second OM micrograph is representative for the structure of tempered specimen C1 and is illustrated in Fig. 6.
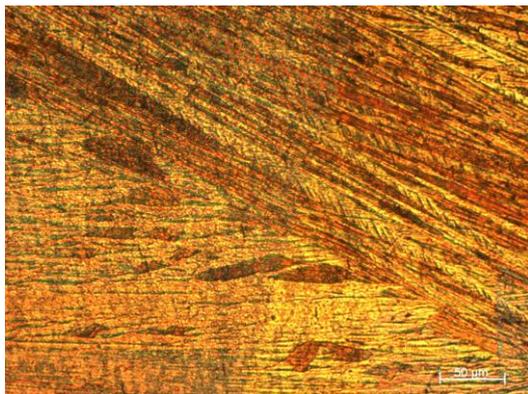
Fig. 6. OM micrograph of 373 K-tempered specimens C1, revealing long parallel martensite plates.

In this case, as well, the structure is martensitic, yet a short comparison between normalized and tempered structures reveals that 373K-tempering caused much longer martensite plates as compared to initial normalized structure.

The last typical OM micrograph corresponds to normalized specimen C2, according to Fig. 7.

In contrast to the other OM micrographs, Fig. 7 reveals the total absence of martensite plates, which seems to confirm the assumptions made when discussing Fig. 4, which did not reveal any evidence of solid state transition. The phase transformation product, which shows no transition within this thermal range, could be bainite, since its nucleation is diffusionless but its growth is diffusion-controlled which could be the cause for the lack of reversibility.
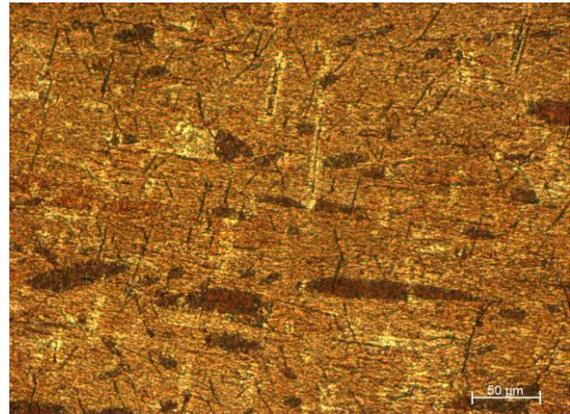
Fig. 7. OM micrograph of 473K-tempered specimen C2, revealing the absence of martensite plates.

In order to prove that the phase transformation product in specimen C2 is bainite, further evidence is necessary. Therefore, for a better insight on C2 structure, Fig. 8 shows an OM micrograph with larger magnification
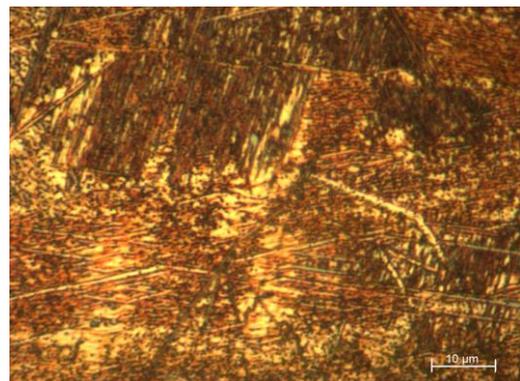
Fig. 8. Magnified OM micrograph of 473K-tempered specimen C2, revealing a series of morphologic characteristics of bainite.

Fig. 8 reveals a plate-like transformation product with internal striations [12] which seem to be irregularly distributed and have the appearance of microtwins [13], which is characteristic to bainite.

Additional evidence of these characteristic morphologic features of bainite was revealed by SEM, in Fig.9.

It is noticeable that bainite plates have extremely fine

internal striations, which could be caused by large dislocations densities [14], and are visible only at very large magnifications, as in Fig.9(b). In good accordance with a previous report which revealed the transitory bainite formation during the tempering of a martensitic Cu-Zn-Al SMA [15], Fig.9 shows a plate-shaped product with morphological characteristics that correspond to bainite [16].
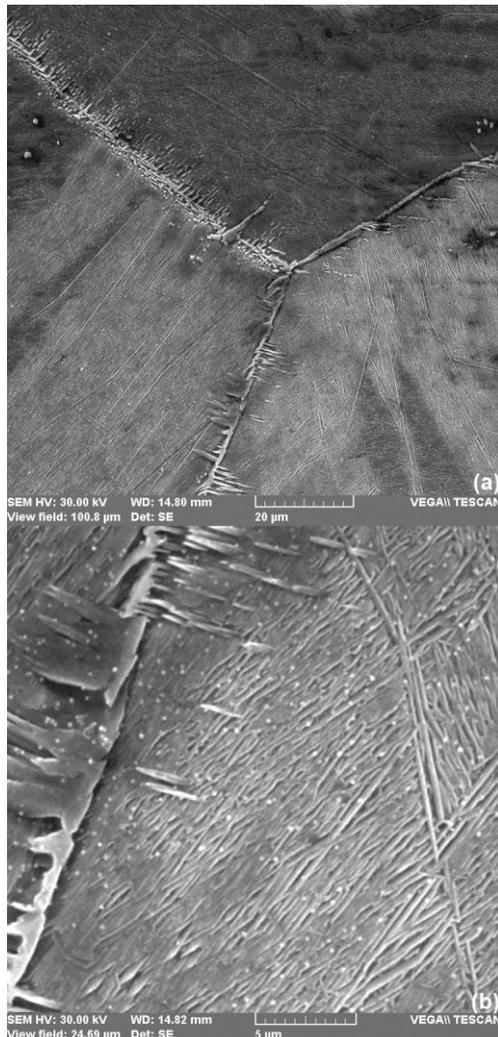
Fig. 9. SEM micrograph of 473 K-tempered specimens C2: (a) intersection area between three crystalline grains; (b) detail of the lower grain boundary, revealing a matrix with characteristic morphologic features of bainite.

4. Conclusions

A reversible stress-induced martensitic transformation has been emphasized by DSC measurements in the case of a normalized hot forged Cu-15 Zn-6 Al (mass. %) SMA. OM micrographs have shown the initial martensitic structure, which is characteristic to this alloy system.

373 K-tempering caused the occurrence of long parallel martensite plates which reverted to austenite to lower temperatures with 4-8 K as compared to normalized

state.

It has been assumed that 473 K-tempering caused the formation of bainite which, due to its diffusion-controlled growth, does not revert to austenite, on heating. Since most of the structural-morphological characteristic features of Cu-Zn-Al bainite were confirmed both by optical and scanning electron microscopy, it can be assumed that the phase transformation product, obtained after 473 K tempering of a normalized Cu-15 Zn-6 Al SMA, is bainite.

References

[1] W. Huang, Mater Design **23**, 11 (2002).
[2] Z. Li, S. Gong, M. P. Wang J Alloy Compd. **452**, 307 (2008).
[3] Z. G. Wang, X. T. Zu, J.H. Wu, L. J. Liu, H. Q.Mo, Y. Huo, J Alloy Compd. **364**, 171 (2004).
[4] L. G. Bujoreanu, N.M. Lohan, B. Pricop, N. Cimpoeşu, J. Mater. Eng. Peform. **20**, 468 (2011).
[5] L. G. Bujoreanu LG, Mater. Sci. Eng. A **481–482**, 395 (2008).
[6] L. G. Bujoreanu, M. L. Craus, I. Rusu, S. Stanciu, D. Sutiman, J. Alloys Compd. **278**, 190 (1998).
[7] L. G. Bujoreanu, M. L. Craus, S. Stanciu, V. Dia, Mater. Sci. Technol. **16**, 612 (2000).
[8] J. Spielfield, Mater. Sci. Eng. **A273–A275**, 639 (1999).
[9] C. M. Wayman, in Shape Memory Effects in Alloys (J. Perkins, ed.), Plenum Press, New York, pp. 1–27 (1975).
[10] Zhu, Wei-Juang, Chen, Wei-Ye, Hsu, T. Y. (Xu Zuyao), Acta metall. **33**, 2075 (1985).
[11] D. W. Wield, E. Gillan, Acta metall. **25**, 725 (1977).
[12] I. Cornelis, C. M. Wayman, Acta metall. **22**, 301 (1974).
[13] J. Spielfield, E. Hornbogen, M. Franz, J. Phys. IV, **C5** 239 (1997).
[14] K. Takezawa, S. Sato, in Proceedings of the International Conference on Martensitic Transformations, ICOMAT-86, The Japan Institute of Metals, Nara, Japan, 625 (1986).
[15] L. G. Bujoreanu, S. Stanciu, P. Bârsănescu, N. M. Lohan, in NM In: Advanced Topics in Optoelectronics, Microelectronics, and Nanotechnologies IV (P. Schiopu, C. Panait, G. Căruntu, A. Manea, eds.), Proc. SPIE Vol. 7297 SPIE, Bellingham, WA, 72970B (2009).
[16] M. H. Wu, C. M. Wayman, in Proceedings of the International Conference on Martensitic Transformations, ICOMAT-86, The Japan Institute of Metals, Nara, Japan, 619 (1986).

_____

*Corresponding author: lgbujor@tuiasi.ro